

# Measurement: Digitalization

## Soil Digitalization Using LED Sensors

--Manuscript Draft--

<b>Manuscript Number:</b>	MEADIG-D-25-00085R1
<b>Full Title:</b>	Soil Digitalization Using LED Sensors
<b>Article Type:</b>	VSI:MEADIG_M4Dconf2025
<b>Keywords:</b>	microsensors; Machine Learning; colorimetry; digitalization; LED; applied geology; seismology
<b>Corresponding Author:</b>	Fabio Leccese Università degli Studi Roma Tre Rome, ROMA ITALY
<b>Corresponding Author Secondary Information:</b>	
<b>Corresponding Author's Institution:</b>	Università degli Studi Roma Tre
<b>Corresponding Author's Secondary Institution:</b>	
<b>First Author:</b>	Federico Fina
<b>First Author Secondary Information:</b>	
<b>Order of Authors:</b>	Federico Fina Massimo Piotto Simone Contardi Fabio Leccese
<b>Order of Authors Secondary Information:</b>	
<b>Abstract:</b>	In this paper, we propose a method of data collection from different sensors through a software developed by Sensichips s.r.l., SLM-Studio, which can then be compared with MLP machine learning models trained through data available on the Sensichips website. The measurements performed by the multispectral SpeCtroscopPe SCP can be applied in different fields of precision agriculture ranging from irrigation water monitoring to the health status of plants and soils up to the monitoring of the chemical-physical conditions of the air.
<b>Additional Information:</b>	
<b>Question</b>	<b>Response</b>
To complete your submission you must select a statement which best reflects the availability of your research data/code. IMPORTANT: this statement will be published alongside your article. If you have selected "Other", the explanation text will be published verbatim in your article (online and in the PDF).  (If you have not shared data/code and wish to do so, you can still return to Attach Files. Sharing or referencing research data and code helps other researchers to evaluate your findings, and increases trust in your article. Find a list of supported	Data will be made available on request.

data repositories in [Author Resources](#), including the free-to-use multidisciplinary open Mendeley Data Repository.)

Dear Editor, Dear Reviewers,

first, we would like to express our personal thanks to the Editor and the Reviewers who helped us to better focus the purpose of our paper. Following the changes requested by the Reviewers, we have reviewed the paper “*Soil Digitalization Using LED Sensors*” taking into account all the details of the reviewers' comments.

We answer separately to the two reviewers:

### **Reviewer #1**

We would like to thank *Reviewer #1* for the constructive comments: they were very helpful for us, so we modified the relevant parts in the revised manuscript to better focus our work. In particular:

- 1) We have improved the quality of the figures in the paper, in particular Fig. 9 and Fig. 17 have been enlarged and we have tried to improve the quality;
- 2) In part III PROPOSAL a section regarding the paper roadmap has been added, we have both explained in points the various experimental steps that have been carried out and inserted an additional figure (Fig. 10) that graphically summarizes the soil digitalization process through the LED sensor.

### **Reviewer #2**

We would like to thank *Reviewer #2* for the constructive comments: they helped us to implement the content of this review. In particular:

- 1) We have corrected Table 2 so that the image and its description are not found on different pages.
- 2) We added the confusion matrices for the MLP and KNN models and a table with the parameters used to train the two models. Finally, in the results section, we specified that the test was validated by performing two separate test measurements on all analyzed soil classes.

(To all the two Reviewers)

Best Regard

Federico Fina, Fabio Leccese

# Novelties respect to the original paper

The original paper, titled “**Soil Digitalization Using Micro-Sensors**” has been presented in the 2025 IMEKO TC-6 International Conference on Metrology and Digital Transformation in Benevento, Italy, September 3-5, 2025. The original paper is uploaded as supplementary file.

The novelties presented in this updated version respect to the original paper are here listed:

- 1) New title: **Soil Digitalization Using LED Sensors**
- 2) **A more in-depth reading on diagnostic investigations for soil characterization (colorimetry, geophysics, seismology, applied geology and geochemistry).**
- 3) **The measurements performed with the SCP multispectral sensor for colorimetry measurements.**
- 4) **Experimental procedures on soil sampling and sieving operations for granulometric analysis.**
- 5) **Data analysis using two machine-learning techniques: MLP and KNN.**

On behalf of the Co-Authors, I affirm that the paper in this new form is completely new and never already published/presented before.

My best Regards

Fabio Leccese

# Declaration of Interest Statement

On behalf of the Co-Authors, I confirm our interest to publish this paper in this Journal within the Special Issue on 2nd International Conference on Metrology and Digital Transformation (M4Dconf), 2025 as a consequence of the fact that the original paper was presented in the 2025 IMEKO TC-6 International Conference on Metrology and Digital Transformation held in Benevento, Italy, September 3-5, 2025.

As additional information, we declare:

- a) This work was co-funded by the European Union Horizon Europe program with the project URBAN M20 (GA 101180710).
- b) AUTHORS' CONTRIBUTION:  
Conceptualization, F.L; methodology, F.F.; validation, F.F. and F.L.; formal analysis, F.F.; investigation, F.F.; data curation, S.C.; writing—original draft preparation, F.F.; writing—review and editing, F.F., F.L., M.P.; supervision, F.L and M.P. All authors have read and agreed to the published version of the manuscript.
- c) As regards the instrumentation, the instrument used was created and developed by Sensichips s.r.l. with funds from the European Union Horizon Europe program with the project URBAN M20 (GA 101180710).

Date, 24/11/2025

Sign

Fabio Leccese

# Soil Digitalization Using LED Sensors

Federico Fina<sup>1</sup>, Massimo Piotto<sup>2</sup>, Simone Contardi<sup>3</sup>, Fabio Leccese<sup>4</sup>

<sup>1</sup>Università Roma Tre Dipartimento di Scienze, Rome (Italy), federico.fina@uniroma3.it

<sup>2</sup>Università di Pisa Dipartimento di Ingegneria dell'Informazione, Pisa (Italy), massimo.piotto@unipi.it

<sup>3</sup>Sensichips.srl, Aprilia (LT, Italy), simone.contardi@sensichips.com

<sup>4</sup>Università Roma Tre Dipartimento di Scienze, Rome (Italy), fabio.leccese@uniroma3.it

**Abstract** – In this paper, we propose a method of data collection from different sensors through a software developed by Sensichips s.r.l., SLM-Studio, which can then be compared with MLP machine learning models trained through data available on the Sensichips website. The measurements performed by the multispectral SpeCtroSCOPE SCP can be applied in different fields of precision agriculture ranging from irrigation water monitoring to the health status of plants and soils up to the monitoring of the chemical-physical conditions of the air.

**Keywords** - microsensors, machine learning, colorimetry, digitalization, LED, applied geology, seismology.

## I. INTRODUCTION

Soil analysis is a topic that encompasses several scientific disciplines, from geology to physics, biology, chemistry, and engineering. The applications of such studies can be manifold, from precision agriculture [1] to the construction of human-made structures to the analysis of the geodynamics of an area of geological interest, such as a riverbed or a beach.

The analogue study techniques are based on the observation of the terrain based on what an expert eye such as that of a geologist or a biologist sees. In recent years interdisciplinary techniques have been developed aimed at the development of different sensors that can be useful both for deepening the studies but also for making the study of the terrain quicker and more accurate. In the case of precision agriculture, the measurements taken by different typologies of sensors can then be transmitted via Wi-Fi [2], ZigBee [3-4] or Bluetooth [5] systems to a sort of central system that is consulted by the farmer, who can decide whether to intervene to reduce the possible onset of problems that can damage the quality and the harvest itself. In the future, these data could be an integral part of a single dataset in which it will be possible to consult the problems of a plant or a vegetable such as the chemical-physical conditions, the type of soil, the meteorological conditions, the soil water content and so on.

Soil is the most superficial layer of the earth's crust and extends from the surface, where there is almost exclusively humus and organic matter, to a layer of the rock, the bedrock, which has a low degree of fragmentation. Each layer of the soil is called a horizon and at the level of nomenclature is named by specific letters as shown in Fig. 1.

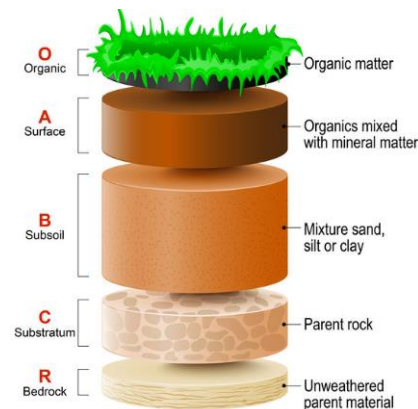


Fig. 1 Geological structure of a soil (Soil is the thin layer of material covering the earth's surface.)

In nature there are different types of soil that are classified based on the granulometry through sieves that evaluate the

# Soil Digitalization Using LED Sensors

**Abstract** – In this paper, we propose a method of data collection from different sensors through a software developed by Sensichips s.r.l., SLM-Studio, which can then be compared with MLP machine learning models trained through data available on the Sensichips website. The measurements performed by the multispectral SpeCtroSCOpe SCP can be applied in different fields of precision agriculture ranging from irrigation water monitoring to the health status of plants and soils up to the monitoring of the chemical-physical conditions of the air.

**Keywords** - microsensors, machine learning, colorimetry, digitalization, LED, applied geology, seismology.

## I. INTRODUCTION

Soil analysis is a topic that encompasses several scientific disciplines, from geology to physics, biology, chemistry, and engineering. The applications of such studies can be manifold, from precision agriculture [1] to the construction of human-made structures to the analysis of the geodynamics of an area of geological interest, such as a riverbed or a beach.

The analogue study techniques are based on the observation of the terrain based on what an expert eye such as that of a geologist or a biologist sees. In recent years interdisciplinary techniques have been developed aimed at the development of different sensors that can be useful both for deepening the studies but also for making the study of the terrain quicker and more accurate. In the case of precision agriculture, the measurements taken by different typologies of sensors can then be transmitted via Wi-Fi [2], ZigBee [3-4] or Bluetooth [5] systems to a sort of central system that is consulted by the farmer, who can decide whether to intervene to reduce the possible onset of problems that can damage the quality and the harvest itself. In the future, these data could be an integral part of a single dataset in which it will be possible to consult the problems of a plant or a vegetable such as the chemical-physical conditions, the type of soil, the meteorological conditions, the soil water content and so on.

Soil is the most superficial layer of the earth's crust and extends from the surface, where there is almost exclusively humus and organic matter, to a layer of the rock, the bedrock, which has a low degree of fragmentation. Each layer of the soil is called a horizon and at the level of nomenclature is named by specific letters as shown in Fig.1.



Fig. 1 Geological structure of a soil (Soil is the thin layer of material covering the earth's surface.)

In nature there are different types of soil that are classified based on the granulometry through sieves that evaluate the percentage of sand, silt and clay present in each soil sample (Fig. 2). Each soil is also associated with a specific color which is characterized according to the granulometry, the mineralogical content and the water content.

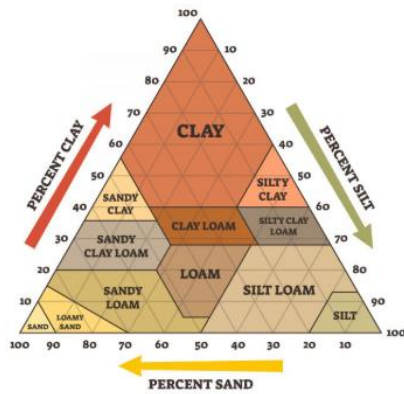


Fig. 2. Soil types classified according to the percentage content of clay, sand and silt (Soil is the thin layer of material covering the earth's surface.)

Field Code Changed

Soil classification is based on grain size and their percentage content in the sample [6], Fig. 2. specifically:

- A sandy soil contains grains with a diameter between 2.0 mm and 0.060 mm, and these grains are clearly visible to the naked eye. In the presence of water, these grains do not form continuous aggregates but separate easily from it [7];
- Silty soil contains grains with a diameter between 0.060 mm and 0.002 mm and retains more water than soils with larger grain sizes [7];
- A clayey soil contains grains with a diameter smaller than 0.002 mm and retain water [7].

These three different granulometries mixed together at different percentage concentrations form different types of soil (Fig. 2): for example there is peaty soil which also contains a good percentage of humus (organic matter), chalky soil which also contains a percentage of gravel (gravel granulometry is greater than 2.0 mm) and loamy soil which is a typically gravelly soil and therefore will contain almost exclusively gravific water, i.e. water which is difficult to retain by the grains.

In literature, soil classification is performed through analog measurements [8], which are time-consuming because several different types of measurements must be performed, such as:

- Caliper and palmer measurements for pebbles larger than 2.0 mm [8].
- Sieve measurements for grain sizes between 2.0 mm and 0.074 mm, and for a good measurement, the sieve must oscillate for at least thirty minutes [8-9].
- Measurements using the aerometric test, which measures the sedimentation rate in water of grains smaller than 0.074 mm [8].

These measurements are often supplemented by further mineralogical analyses, which are performed in laboratory using laser and X-ray analysis [8-10].

The process of digitizing a soil consists of cataloguing the different types of soils in Fig. 2 by creating a database that contains the chemical-physical, geological, mechanical, electrical, optical properties of each soil class.

The aim of the following article is therefore to find a technique that allows the digitalization of parameters characterizing different types of soils by creating datasets that combine measurements from sensors with machine learning algorithms that can speed up the process of recognizing.

After a brief presentation on the instruments used in different geological fields for soil study, the paper will present a multispectral sensor developed by the microsensor company Sensichips s.r.l. [11] called SectrosCoPe (SCP). This sensor can be used to perform imaging with LEDs of various wavelengths and it is possible to use this instrument for the recognition of the various types of soil by means of machine learning algorithms.

1  
2  
3  
4  
5  
6  
7  
8  
9  
10  
11  
12 **II. STATE OF THE ART**

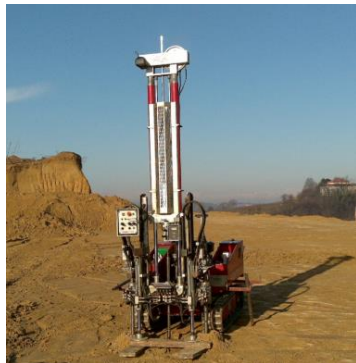
13 In soil analysis, there are different types of sensors that incorporate different scientific technical knowledge such as  
14 geophysics, chemistry, biology, etc. up to electronic and telecommunications engineering. Creating a digital database of  
15 a terrain requires knowledge of a series of diagnostic techniques that will be addressed in the following paragraph.

16 **A. GEOGNOSTIC INVESTIGATIONS**

17 Geognostic surveys encompass a series of techniques that investigate the subsoil through excavations and mechanical  
18 drilling. Their purpose is to extract soil for sampling and laboratory analysis, reconstructing, for example, the stratigraphy  
19 of a subsoil. This can be used for various purposes: stratigraphy, water wells, construction site surveys, and more [12].

20 Alongside these sampling operations, there are diagnostic investigations aimed at studying the mechanical properties of  
21 a soil. Among these, we can mention:

- 22 - The conical tip penetrometer test [13] (CPT, Fig. 3), which can reach depths of up to 30 m, is performed on  
23 granular soils or soft cohesive soils. This technique involves continuously penetrating the soil with a conical tip,  
24 which measures the penetration resistance at the tip ( $R_p$ ) and the lateral friction ( $R_L$ ) via the lateral sleeve (or  
25 friction jacket). The  $R_p/R_L$  ratio provides information on the soil's grain size. Furthermore, if the tip is equipped  
26 with a piezocone, information on the soil's pore pressure can also be obtained (this test is called CPTE).
- 27 - The dynamic penetration test (SCPT) [14], which can reach a depth of 25 m and can be applied to any type of  
28 soil, provides an indirect measurement of soil resistance. This technique involves continuously penetrating the  
29 soil using a drill bit driven by a 73 kg hammer that dropped from a height of 75 cm. In a 30 cm segment, the  
30 number of blows ( $N_{SPT}$ ) needed to sink the rod using the standard penetration test (SPT) technique and the  
31 number of blows needed to penetrate the conical drill bit ( $N_p$ ) 30 cm are diagnostic for different soil types.



42 *Fig. 3 Conical Penetrometer Test (CPT)*

43 **B. GEOELECTRIC SURVEYS**

44 Geoelectricity is one of the soil diagnostic techniques that can be used to detect the possible presence of water within soil  
45 [15], the presence of solid minerals important for the mining industry, and the geoelectric properties of a terrain [16]. The  
46 techniques [17] that will be discussed use Ohm's law  $R=\rho L/A$  where L is the length of the line being analyzed, A is the  
47 cross-section, and  $\rho$  is the resistivity of the soil block. In general, the device most used in geoelectric is composed of four  
48 electrodes, two of which are current-carrying and connected to a battery and an ammeter, while the other two are  
49 measuring electrodes connected to a galvanometer (Fig.4). Under the circuit conditions just described, the resistivity is  
50 equal to  $\rho=K \Delta V/I$  where I is the current, V is the potential, and K is a coefficient that depends on the distance between  
51 the electrodes. By increasing the distance between the electrodes, it is possible to increase the depth to which the soil can  
52 be analyzed. Resistance is therefore a diagnostic data to discriminate the different types of soil. The two devices used for  
53 geoelectrical surveys are:

- 54 - In Wenner's device [18-19] the distance between the electrodes is fixed at a certain value  $a$  and therefore the
- 55  
56  
57  
58  
59  
60  
61  
62  
63  
64  
65

resistivity of the ground will be equal to  $\rho = 2\pi aK V/I$ . This technique can be used to discriminate lateral variations in the terrain.

- In the Schlumberger device [20], the distance  $b$  between the measuring electrodes is smaller than the distance  $c$  between the current electrodes. These are symmetrically moved towards the outside of the device with the aim of monitoring the vertical variations of the ground from a geoelectrical point of view. The resistivity in this case is equal to  $\rho = \pi \frac{V c^2 - b^2}{I ab}$

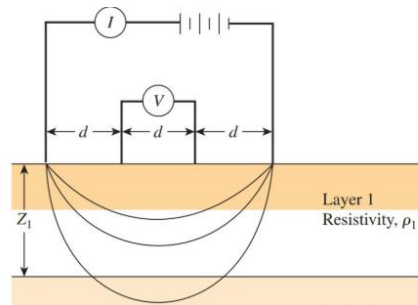


Fig. 4 Circuit diagram of a sensor used in geoelectrics

Furthermore, geophysical sensors are also mainly applied for monitoring the first horizons of the soil. At a theoretical level, geophysical sensors analyze two types of waves: electromagnetic waves or acoustic ones. As examples of the first category, there are the Ground Penetrating Radar (GPR) [21] and the three-wire probe connected to a Vector Network Analyzer (VNA) [22]. Instead, with the use of GPR from the interaction of the waves with the dielectric properties of water, from the analysis of the reflected signal it is possible to analyze the water content of the soil and the soil horizon in which it is located [23-24].

### C. GEOSEISMIC INVESTIGATIONS

Geoseismic surveys [25] exploit the elastic properties of the ground by studying its oscillations [26-27] through active seismic measurements, which use explosives, and passive seismic measurements [28], which record earthquakes and seismic noise in the ground. Geoseismic surveys of a soil [29] can be conducted to analyze its porosity, water content, and rheology. Furthermore, it is possible to investigate the grain size of a soil by studying the propagation velocities of compressional waves, known as P-waves. The circuit diagram of an instrument used for active seismic surveys (Fig. 5) is as follows:

- A seismic source that generates compression waves. This source can be either a ground impact or an explosive;
- A receiver that generates a current through the mechanical oscillation of an inductor in a magnet;
- A series of amplifiers that amplify the weak signal coming from the receiver by a factor of 10000-1000000;
- A system of controls that filter the frequency signal, cutting out external disturbances such as wind, traffic, power lines, etc;
- Recorder that acquires the signal digitally with a sampling rate of the order of ms.

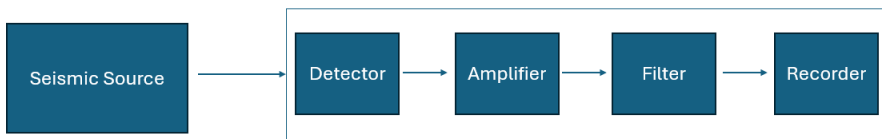


Fig. 5 Seismic Sensor circuit

An example of a seismic sensor is the Lennartz-3D-5s. This is a mechanical sensor that allows quantitative analysis of

1  
2  
3  
4  
5  
6  
7  
8  
9  
10 the seismic noise of any type of terrain.

11 This sensor can be used both to perform a diagnostic investigation of the seismic response of the ground (through H/V  
12 analysis, the ratio between the horizontal and vertical signals [30]), in which the resonance peak can be identified, and to  
13 perform a quantitative analysis of the water content within the ground [31].

#### 14 D. GEOCHEMICAL INVESTIGATIONS

15 Chemical sensors instead work mainly in monitoring the chemical-physical characteristics of agricultural soil.  
16 Temperature [32-33], pH [34], humidity [35] and conductivity meters [36] are available on the market as gas detectors  
17 [37]. The parameters just mentioned can be applied both in monitoring the water with which the fields are irrigated, and  
18 to monitor horizon A of a soil and to monitor the atmospheric environment in which the crop is located. In recent years,  
19 the microelectronics industry is developing smart micro sensors that can be applied to the world of precision agriculture  
20 and through machine learning techniques it is possible to reveal chemical anomalies of the soil or of the leaves themselves  
21 even before the effects are perceptible by the human eye [38-39].

#### 22 E. SPECTROSCOPIC INVESTIGATIONS

23 The optical sensors available on the market exploit different forms of material radiation interaction such as reflectance  
24 [40], transmission [41] and fluorescence [42] of a given substance. This technique is applied through different portable  
25 spectrophotometers that work in different ranges of the electromagnetic spectrum: from ultraviolet (UV), to visible (VIS)  
26 [43] up to near infrared (NIR) [44]. The different spectroscopic techniques help us to discriminate, for example the  
27 presence of microfungi substances on the surface of a leaf as well as the health status of the plant [45]. Fluorescence, for  
28 example, is a technique that allows us to observe the water content of a leaf and therefore can provide interesting data on  
29 its hydration [46]. Another important type of optical sensors available on the market are colorimeters that can be applied  
30 in different fields such as monitoring the health status of a leaf [47-48] or the color of a soil [49] which is also a diagnostic  
31 element of a soil.

### 32 III. PROPOSAL

33 As seen in Section II, soil classification is based on various diagnostic techniques of different disciplines such as applied  
34 geology, seismology, geophysics, and materials science [50]. When we talk about digitizing soil, we mean creating a sort  
35 of directory where each soil class has subfolders with very specific properties. For example, we can say that a sandy soil  
36 has two completely different grain sizes compared to a clay soil: sand has grains in the order of millimeters, while clays  
37 have micrometer grains [51]. These grains form a soil, creating a sort of network of grains held together by contact forces.  
38 Void zones form between the grains, providing an important piece of data: the soil's porosity is defined as the ratio  
39 between the total volume of the pores and the total volume of the grains ( $\Phi = V_{pores}/V_{solid}$ ).

40 A clay soil has a greater porosity than a sandy soil, but a completely different permeability,  $K$ . This is the ability of a soil  
41 to drain water and depends on the rheology of the soil, its porosity, and how the voids communicate [50]. Clay has a  
42 relatively high porosity, but the voids are very small and do not communicate with each other, making clay soil  
43 impermeable, unlike sandy soil, which is permeable. The geognostic tests mentioned in paragraph II.A allow us to classify  
44 soils based on their mechanical properties; in particular, the  $R_p/R_L$  and  $N_{SPT}/N_p$  ratios provide data on how different soil  
45 types are resistant to mechanical penetration [52]. The geoelectrical tests described in section II.B provide data on a  
46 possible classification of soils based on how an electromagnetic field interacts with a soil, providing data such as the soil's  
47 electrical resistance to the flow of a current [53]. The seismic tests II.C, on the other hand, provide data on the resonance  
48 frequency of a particular soil class and the propagation velocity of seismic waves ( $v_p$  for P waves or compression waves,  
49  $v_s$  for S waves or shear waves) [54]. These velocities depend on the rheological properties of the soil and therefore on its  
50 elastic properties.

51 Some of the chemical-physical properties of the soils have been inserted in Fig. 6 which must be seen as a sort of rubric  
52 in which each box represents a soil typology with a series of diagnostic chemical-physical characteristics for the  
53 classification inside [50].  
54  
55  
56  
57  
58  
59  
60  
61  
62  
63  
64  
65

1  
2  
3  
4  
5  
6  
7  
8  
9  
10  
11  
12  
13  
14  
15  
16  
17  
18  
19  
20  
21  
22  
23  
24  
25  
26  
27  
28  
29  
30  
31  
32  
33  
34  
35  
36  
37  
38  
39  
40  
41  
42  
43  
44  
45  
46  
47  
48  
49  
50  
51  
52  
53  
54  
55  
56  
57  
58  
59  
60  
61  
62  
63  
64  
65

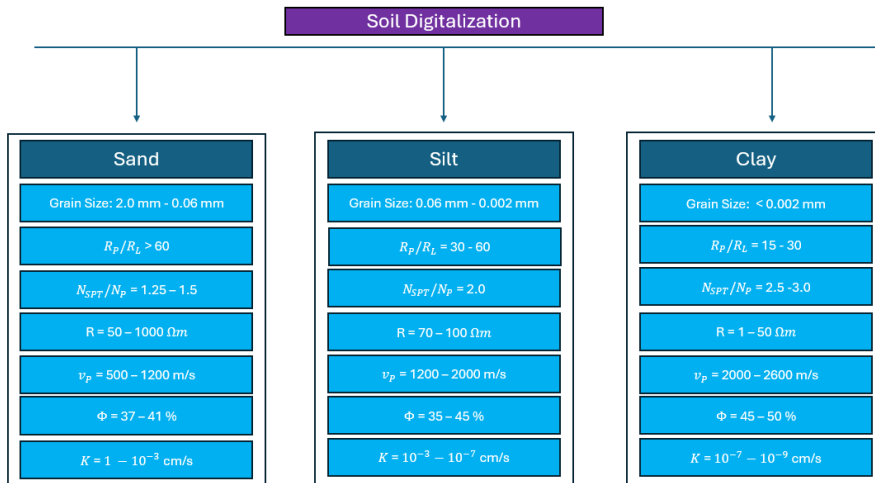


Fig 6. In this figure you can see how we intend for soil digitalization. Each soil can be thought as a table with different properties.

In addition to these properties, those investigated in this paper include optical properties, which depend on the soil's grain size [55], its mineralogical content, and, above all, its water content [56]. This is an important and discriminating factor for some of the properties, such as seismic, geoelectric, and mechanical properties. Based on the literature review, soil colorimetry is performed using colored analog tablets that contain a vast catalog of colors that are part of the Munsell diagram [57]. Field color measurements are analog measurements performed by placing the soil sample next to a possible color from the catalog, and based on the association made by the operator, that soil type is associated with a specific color code. Obviously, this technique, while valid, has some weaknesses, such as the fact that soil classification based on a given color can be disturbed by the operator himself, who may have a visual system more sensitive to some color tones than others. The aim of the paper is therefore to add the optical properties of the soils Fig. 7 and analyze their colorimetry, creating a database suitable for digitizing the different classes of soil under examination.

1  
2  
3  
4  
5  
6  
7  
8  
9  
10  
11  
12  
13  
14  
15  
16  
17  
18  
19  
20  
21  
22  
23  
24  
25  
26  
27  
28  
29  
30  
31  
32  
33  
34  
35  
36  
37  
38  
39  
40  
41  
42  
43  
44  
45  
46  
47  
48  
49  
50  
51  
52  
53  
54  
55  
56  
57  
58  
59  
60  
61  
62  
63  
64  
65

Soil			
	Sand	Silt	Clay
Colorimetry	Grey, White, Red	Grey, Red	Red
Granulometry	Grain Size: 2.0 mm - 0.06 mm	Grain Size: 0.06 mm - 0.002 mm	Grain Size: < 0.002 mm
Seismology	$v_p = 500 - 1200$ m/s	$v_p = 1200 - 2000$ m/s	$v_p = 2000 - 2600$ m/s
Electric Properties	$R = 50 - 1000 \Omega m$	$R = 70 - 100 \Omega m$	$R = 1 - 50 \Omega m$
Mechanical Properties	$R_p/R_L > 60$	$R_p/R_L = 30 - 60$	$R_p/R_L = 15 - 30$
	$N_{SPT}/N_p = 1.25 - 1.5$	$N_{SPT}/N_p = 2.0$	$N_{SPT}/N_p = 2.5 - 3.0$
Hydrological Properties	$\Phi = 37 - 41 \%$	$\Phi = 35 - 45 \%$	$\Phi = 45 - 50 \%$
	$K = 1 - 10^{-3}$ cm/s	$K = 10^{-3} - 10^{-7}$ cm/s	$K = 10^{-7} - 10^{-9}$ cm/s
	...	...	...

Fig 7. Mechanical, colorimetric, seismic, electrical and hydrological properties of soils are summarised in a table which should be seen as a section in which each type of soil opens into sub-folders in which the different mechanical, geophysical, chemical and optical properties are summarized

Furthermore, since colorimetric analyses are based on the study of the signal reflected by a hypothetical soil, they also consider the water content present on its surface [56]. This water interacts with the grains, initially creating a small film that covers the grain surface (pellicular water), which then grows larger, interacting first with the nearest grains (pellicular water) and then with the entire system (gravitational water). This latter configuration is very important in hydrogeology [58], as it is the water that can be extracted from an aquifer. Gravitational water, unlike pellicular and capillary water, which respond to Coulomb electrostatic attraction, responds to the gravitational law  $F = mg$  and so it is therefore the water that percolates within the soil. Optically [55], water is an absorbing medium that obeys the Beer-Lambert law

$$R = R_d e^{-\alpha d} \quad (1)$$

where  $\alpha$  is the absorption coefficient of a given substance and  $d$  is the optical path. Since our substance is a mix of water and sand, the spectral reflectance must consider both these components and equation 1 can be rewritten as:

$$R = f_s R_d e^{-\alpha d} \quad (2)$$

where  $f_s$  describes the contribution of elastic scattering to reduction of spectral reflectance upon wetting, while parameter  $d$  (optical path length in water) describes the contribution of absorption to reduction of spectral reflectance upon wetting.

Therefore, the reflectance of the signal tends to decrease as the soil water content increases (Fig. 8, Fig. 9). This implies that an accurate colorimetric investigation includes the optical analysis of the soils even when the water content varies.

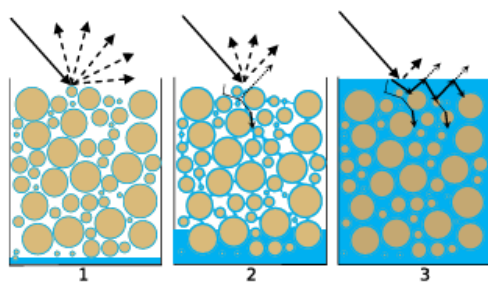


Fig. 8 Interaction between electromagnetic radiation and sand, as can be observed by increasing the water content within the sample being analyzed, the light is not only reflected but also absorbed, thus reducing the amount of the reflected signal [55].

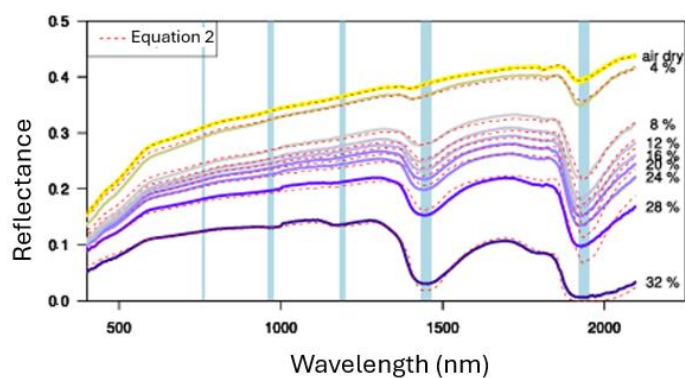


Fig. 9 Reflectance spectrum of sandy soil in the VIS and NIR. Increasing the water content the reflectance decreases [55].

As can be observed in Fig. 9 the reduction of reflectance of a sandy soil analyzed in [55] decreases with increasing water content throughout the spectrum from VIS to NIR. In this work we propose to study soils both in anhydrous conditions and in conditions of soil saturated with water.

Experimentally, the following article was structured as follows (Fig. 10):

- The first phase of the work focused on a series of soil samples taken in the field at various locations in the metropolitan area of Rome. The sampling sites were chosen based on the outcrops catalogued on the geological maps of the Roman area;
- The soil samples were pre-analyzed in the laboratory through sieving operations that made the samples uniform in grain size, and the grain size analyses allowed for the geological classification of the soil;
- The samples were analyzed with the multispectral sensor, the spectroscope SCP, to analyze individual samples from a colorimetric perspective;
- The collected data were analyzed with a neural network that allowed for the creation of an algorithm capable of classifying the soil from a grain size perspective based on colorimetric measurements.

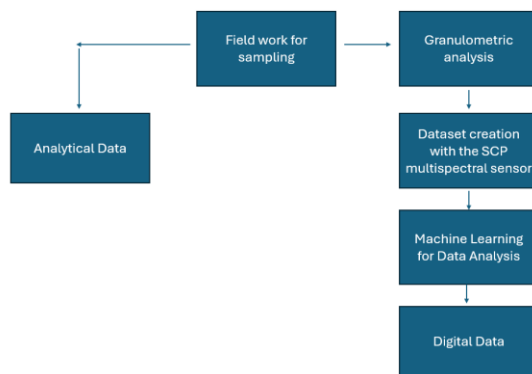


Fig. 10 A conceptual map that represents the underlying theme of the paper. Here you can see how analytical data was transformed into digital data.

#### IV METHODS

The company Sensichips s.r.l. has developed several micro sensors that can be applied in different agricultural fields by providing a data set that can be found online on the website [11]. These sensors are:

- The Air Sensor (SCA) which can monitor air quality, the presence of pollutants, and the presence of flammable gases. The sensor can also monitor ambient temperature and humidity.
- The Water Sensor (SCW) can monitor water quality and the presence of pollutants. Furthermore, the sensor can monitor ambient temperature, pH and humidity and it can be used for both water and wastewater analysis.
- The Multispectral Sensor, the Spectroscope (SCP) is a multispectral sensor that is used in colorimetric fields to monitor the health of plants, the quality of food, as well as the colorimetry of soils.

The sensors include an ASIC (Application-Specific Integrated Circuit), the SENSIPLUS [38], which is a programmable electronic interface developed by the Sensichips in cooperation with the University of Pisa. The interface performs voltage and current measurements and Electrochemical Impedance Spectroscopy (EIS) using two or four contact configurations.

The SCP multispectral sensor, shown in Fig. 11, features 12 LEDs covering most of the VIS to NIR spectrum, as shown in Fig. 12, and an SFH-2201 photodiode as a detector. The sensor operation is based on the emission of a discrete frequency modulated signal by each single LED on the SCP that is reflected by a colored target such as a leaf or a soil sample and then analyzed by a photodiode that converts it into a current signal. In particular, two current components, one IN-PHASE and one 90° phase-shifted QUADRATURE with respect to the stimulating signal, are measured by the photodiode for each LED source.

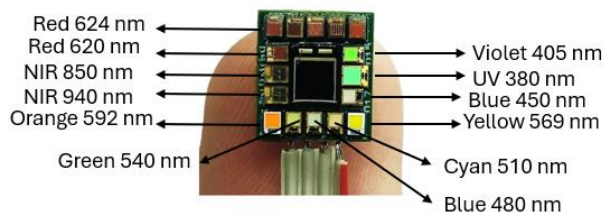
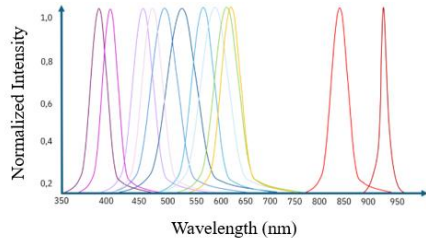


Fig 11. SCP multispectral sensor for soil colorimetry. The arrows show the wavelength associated to each LED.

Any LED can be used for light emission while the measurement can be performed with any other LED or photodiode.



Light emission and measurement can be performed with a lock-in amplifier modulation at a user-programmable frequency, both in-phase and quadrature components can be acquired. The use of the lock-in technique helps to reduce ambient light interference on the measurement.

Fig. 12. Emission spectrum of the 12 LEDs placed on the SCP multispectral sensor. As can be observed, they cover a large part of the VIS (10 LEDs) and a part of the NIR between 800 nm and 950 nm.

The SCP is connected to the PC via a COM-USB port connected to an ESP32 microcontroller (Fig. 13) and the 12 signals acquired by the photodiode are collected by 12 OUTPUTS summarized in the following table (Tab. 1).

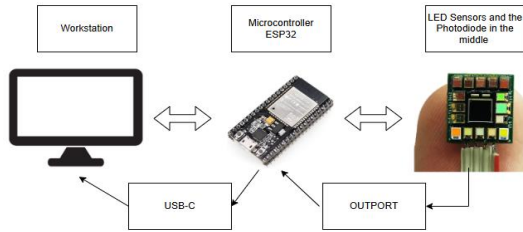


Fig. 13 Schematic view of the experimental setup.

<b>OUTPUT</b>	<b>Wavelength (nm)</b>	<b>Color</b>
Drive0	405 nm	Violet
Drive1	380 nm	UV
Drive2	450 nm	Blue
Drive3	569 nm	Yellow
Drive4	510 nm	Cyan
Drive5	480 nm	Blue
Drive6	540 nm	Green
Drive7	592 nm	Orange
HP_VF2VS	940 nm	IR
HP_DF2DS	850 nm	IR
AUX	620 nm	Red
SHA	624 nm	Red

Tab. 1 Summary table of the 12 OUTPUTS present on the SCP. Each OUTPUT is associated with an LED with a given wavelength and therefore a given color.

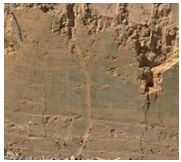
V MATERIALS

After conducting a brief geological survey of the outcrops present in Lazio (Progetto CARG Lazio, ISPRA Ambiente [59]), several sites were selected for soil sampling.

For the purposes of this paper, several soil samples with varying textures and grain sizes were collected. Specifically, coarse sands, fine sands, silts, and clays from the fluvial deposits of the Tiber River (Rome, Italy [60]) and the beaches of Fiumicino (Rome, Italy [61]) and Torvaianica (Rome, Italy [62]) in Lazio were analyzed (Fig. 14). Tab. 2 provides the types of soil sampled, a brief geological description of the sample, and the site where the sampling was performed.

<b>SAMPLE</b>	<b>Description</b>	<b>Location</b>
<p><i>Fine Sand</i></p> 	<p><i>Gray and yellowish quartz sands, rich in volcanic minerals and magnetite. Thickness 1.0–10 m (Holocene).</i></p> <p><i>387 Albano Laziale [62]</i></p>	<p><i>Torvaianica (RM, Italy)</i></p>
<p><i>Medium Sand</i></p> 	<p><i>Loose sands, medium-coarse to medium-fine, composed of quartz, feldspar, pyroxene, and abundant iron minerals. Grain size and composition also influenced by the presence of the Tiber River (Pleistocene-Holocene).</i></p> <p><i>386_FIUMICINO [61]</i></p>	<p><i>Fiumicino (RM, Italy)</i></p>
<p><i>Coarse Sand</i></p> 	<p><i>Coarse sand containing gravel of volcanic origin from the Monti Sabatini volcanic district.</i></p> <p><i>Part of the grains are of igneous origin from the Tolfa mountains.</i></p>	<p><i>Santa Marinella (RM, Italy)</i></p>
<p><i>Loam</i></p> 	<p><i>Silty-sandy and silty-sandy deposits of alluvial plains. These consist of alternating sands, silts, clays, and organic-rich layers up to 10 m thick (Holocene).</i></p> <p><i>374_ROMA [60]</i></p>	<p><i>Quartier Ferratella (RM, Italy)</i></p>
<p><i>Silt</i></p> 	<p><i>Fluvial sediments from the Tiber River from the Magliana district of Rome (Italy)</i></p> <p><i>374_ROMA [60]</i></p>	<p><i>Quartiere Magliana (RM, Italy)</i></p>

1  
2  
3  
4  
5  
6  
7  
8  
9  
10  
11  
12  
13  
14  
15  
16  
17  
18  
19  
20  
21  
22  
23  
24  
25  
26  
27  
28  
29  
30  
31  
32  
33  
34  
35  
36  
37  
38  
39  
40  
41  
42  
43  
44  
45  
46  
47  
48  
49  
50  
51  
52  
53  
54  
55  
56  
57  
58  
59  
60  
61  
62  
63  
64  
65

<p>Clay</p> 	<p>Fluvial sediments from the Tiber River from the Magliana district of Rome (Italy) 374_ROMA</p>	<p>Quartiere Magliana (RM, Italy)</p>
---	---	---------------------------------------

Tab. 2 Summary table of the soil samples. Here you can read a brief description of the analyzed outcrop, the sampling location, the ISPRA reference map, and possible dating. The dating data was taken from the geological map; no further laboratory analyses were performed.

Given that these soils consist of different grain sizes; to perform a rigorous quantitative analysis of the soils shown in Fig. 7 and in Fig.10, it was decided to use experimental methods for soil grain size analysis with the support of the Geophysics Laboratory of the University of Roma Tre (Fabio Cammarano) and the Hydrogeology Laboratory (Roberto Mazza).



Fig. 14 Fine sand sample at the top and coarse sand sample at the bottom.

After being dried in an oven at 105 °C to eliminate moisture and thus the hygroscopic water present on the grain surfaces, the samples were processed using sieves (see Fig. 15). These consist of a series of cylinders numbered with a sieve code that are stacked one on top of the other so that the device, through its mesh, first retains the largest grain sizes and then collects only the fine fraction. Sieves are typically used to analyze the sandstone component of soils, and therefore grain sizes ranging from fine gravel (sieve N. 2) to the boundary between silt and clay (sieve N. 200).

After weighing the net weight of the dried sample  $W_s$ , it was placed inside an American sieve (ASTM) [50], which consists of a series of sieves arranged in decreasing order of fineness. The sieve is rotated and oscillated for approximately 12 minutes to select the various grain size components of the soil: fine gravel, coarse sand, fine sand, silt, and clay.



Fig. 15 A sieve used for sifting soil. The sieving time was set to 12 minutes to sift the different grain sizes evenly.

Once the operation was completed, the individual sieves were weighed with the retained soil and the net weight and percentage of retained soil were calculated. The total weight of the grains present in the sieve at the end of the sieving process was different from the weight of the dried soil at the start because during the sieving process the sample absorbed part of the humidity from the external environment which adhered to the surface of the grains in the form of hygroscopic water. The percentage of soil retained [50] by the single sieve is equal to

$$P = 100 \frac{W_s - \sum W_t}{W_s} \quad (3)$$

where  $W_t$  is the weight of the material retained by all the sieves with a diameter equal to or greater than that of the sieve being analyzed (Fig. 16).



Fig. 16 Gross weight weighing operation sieve with soils inside.

To facilitate the measurement of the mass of the soil grain size fraction, the sieve's tare weight was measured for each individual sieve before starting the sieving process and the gross weight of the sieve-soil system retained after the 12 minutes of sieving with the machine shown in Fig. 16.

The data for the Torvaianica sand sample are shown in the following table Tab. 3. For the sake of completeness, it should be emphasized that the uncertainty associated with the mass of the empty sieve and the full sieve is equal to 0.01 g, i.e. the last digit of the electronic scale used (Fig. 16), while the mass of the net weight of the soil retained in the sieve is equal to  $u_f = \sqrt{0.02}$  (this value comes from the operation of propagation of uncertainties).

sieve diameter ( $\mu\text{m}$ )	sieve mass (g)	Total mass (g)	retained soil mass (g)
2000	387.26	415.42	28.16
1250	369.04	489.98	120.94
600	315.18	691.57	376.39
425	293.86	636.65	342.79
250	284.28	932.63	648.35
125	274.26	499.38	225.12
75	256.21	299.8	43.59
45	264.82	297.42	32.60
Final Box	245.07	253.97	8.90
		Total	1826.84

Tab. 2 Summary result of the sieving operations carried out in the laboratory.

Once the measurements of the masses of the materials retained in the sieves were completed using the formula (3), the following graph (Fig. 17) was obtained where the diameter of the grains is shown on the abscissa and the percentage of mass retained by the sieves is shown on the ordinate (obviously starting from sieves with larger meshes to those with smaller meshes).

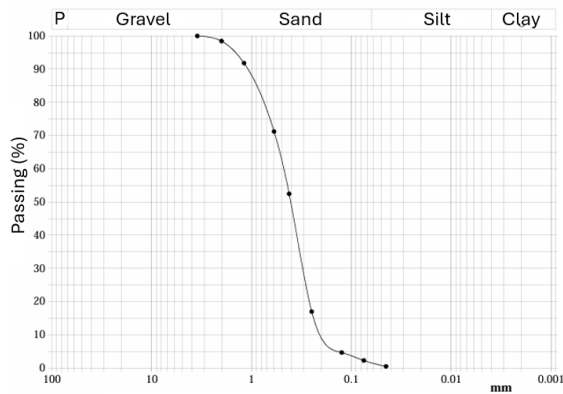


Fig. 17 Final result of sieving, graph with percentage of soil passing through the sieves.

As can be seen in Fig. 17, the curve shows a vertical trend near the sand. This implies that the sieves with mesh diameters equal to those of the sand retained higher percentages of soil during the sieving operations.

At this point, to classify the soil and place it in a graph like Fig. 2, the percentage of soil passing through the 2 mm sieve (gravel) and the percentage of the last sieve on the silt-clay boundary were calculated from the experimental graph Fig. 14. From these, the following experimental graph was obtained and shown in Fig.18.

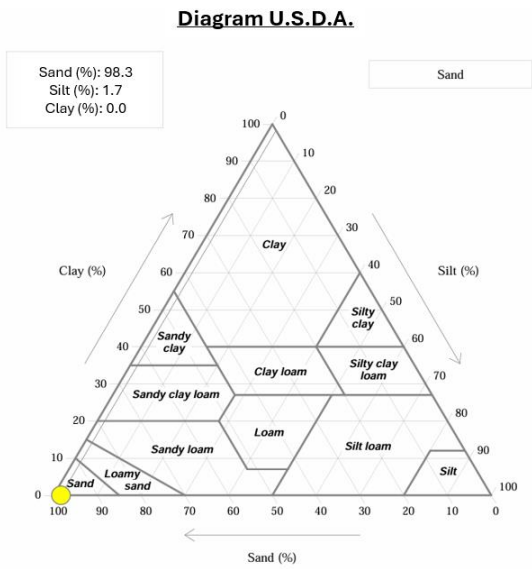


Fig. 18 Classification of the analyzed soil sample.

As can be seen in Fig. 18, the sample taken from Torvaianica is a fine sand containing small percentages of silt and clay. In this type of soil, having a mass passing through the final sieve less than 12% of the total mass of the analyzed soil, the anemone test to calculate the percentage of silt and sand present in the sample was not necessary as it did not discriminate for the purposes of classifying the soil under examination.

This operation was repeated for all the Tab. 2 soils analyzed in this paper.

#### VI MEASUREMENTS AND RESULTS

Once the sieving phase was completed, the samples were placed inside special plastic bags to minimize the possibility of the sample being altered by ambient humidity. At that point, an experimental setup suitable for colorimetric measurements with the SCP was set up in the Electrical and Electronic Measurements Laboratory of the Department of Sciences of the University of Roma Tre (Fabio Leccese). To minimize ambient noise due to external lights (solar, laboratory neon lamps, ...), the SCP was placed inside a black box and placed on a rigid cardboard board, also black. This was positioned on a 5.0 cm raised rail, and the sample being analyzed was placed inside the darkroom. To allow the SCP inside the box to communicate with the workstation, a small hole was made on the surface of the box so that the COM-USB (Fig. 19) port connected the PC to the ESP32.

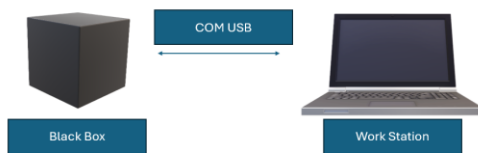


Fig. 19 Experimental setup with the black box inside which the SCP was placed, the COM-USB that connects the instrument to the workstation and the PC.

1  
2  
3  
4  
5  
6  
7  
8  
9  
10 The measurements were performed using the software developed by Sensichips, SLM-Studio, which allows data to be  
11 collected from different sensors in a single device. The device communicates with the various sensors via a Wi-Fi or a  
12 COM-USB system that collects the measurements from the various sensors and communicates them to the PC in which  
13 the SLM-Studio software is present for data analysis. The measurements are driven through different measurement  
14 batches where alternating current and frequency modulated inputs are provided to the sensor and the collected data is  
15 inserted into a Zip folder containing an Excel file.

16 Each Excel file will contain a set of numerical data associated with the measurements of each individual sensor. For each  
17 substance, in this case for each soil type analyzed, a series of spectrophotometric measurements were performed. When  
18 combined, these measurements will describe a specific class (sandy soil, silty soil, etc.). Once this phase is complete,  
19 SLM-Studio can perform data analysis by creating two machine learning models: Multi-Layer Perceptron (MLP) and K-  
20 Nearest Neighbours (KNN) [63-64]. These models can then be tested both with test measurements and by replicating the  
21 same experimental conditions as the training, as well as by making small modifications to the experimental setup. The  
22 operating logic of the SLM-Studio software, created and developed by Sensichips s.r.l. [11], with its three work blocks  
23 (Measurements, Machine Learning, Tests), is shown on Fig. 20.

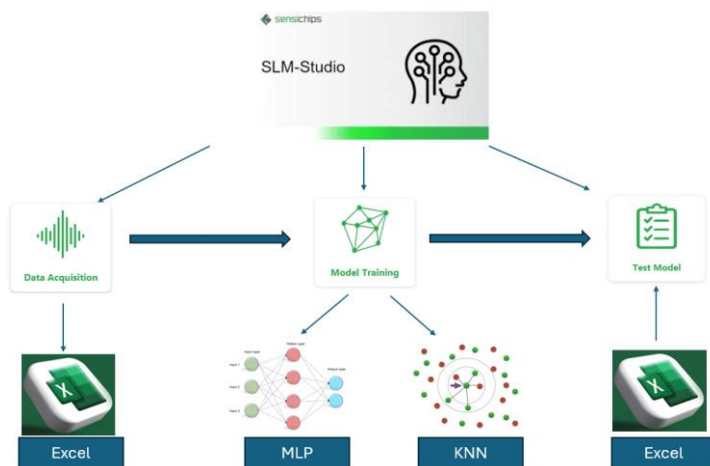


Fig. 20 Schematic of how SLM-Studio works

39 The following paragraphs will explain the measurement techniques performed with the SCP using SLM-Studio (Data  
40 Acquisition), the data processing techniques with machine learning algorithms (Model Training) and the subsequent phase  
41 of testing the created models (Test Model).

#### 42 A. DATA ACQUISITION

43 For the training measurements, regardless of the sensor used, the following methodology was used (Fig. 19):

- 44 - The SCP has been allocated inside the black box to reduce the ambient noise associated with the light inside the  
45 laboratory.
- 46 - Then the measurement starts and for the first 51 repetitions the sensor measured the ambient background noise  
47 inside the black box.
- 48 - After observing that the noise had a stable trend over time, the substance was inserted inside the black box at 5.0  
49 cm from the SCP.
- 50 - After that, the measurement continued for other 99 repetitions until the end of the measurement cycle.

51 Furthermore, to have a complete database for each soil class analyzed, 5 measurements were performed in dry soil  
52  
53  
54  
55  
56  
57  
58  
59  
60  
61  
62  
63  
64  
65

1  
2  
3  
4  
5  
6  
7  
8  
9  
10  
11  
12  
13  
14  
15  
16  
17  
18  
19  
20  
21  
22  
23  
24  
25  
26  
27  
28  
29  
30  
31  
32  
33  
34  
35  
36  
37  
38  
39  
40  
41  
42  
43  
44  
45  
46  
47  
48  
49  
50  
51  
52  
53  
54  
55  
56  
57  
58  
59  
60  
61  
62  
63  
64  
65

conditions and 5 measurements in wet soil. This choice was made because the colorimetry of a granular material depends both on the chemistry of the compound and on its water content. In Fig. 21, the different spectral response of the sample to varying incident light and water content can be observed for each soil type. In Fig. 21 a sand sample taken from the beach of Torvaianica (Rome, Italy) was analyzed which at the mineralogical level is mainly formed by carbonates, quartz and k-feldspar [65].

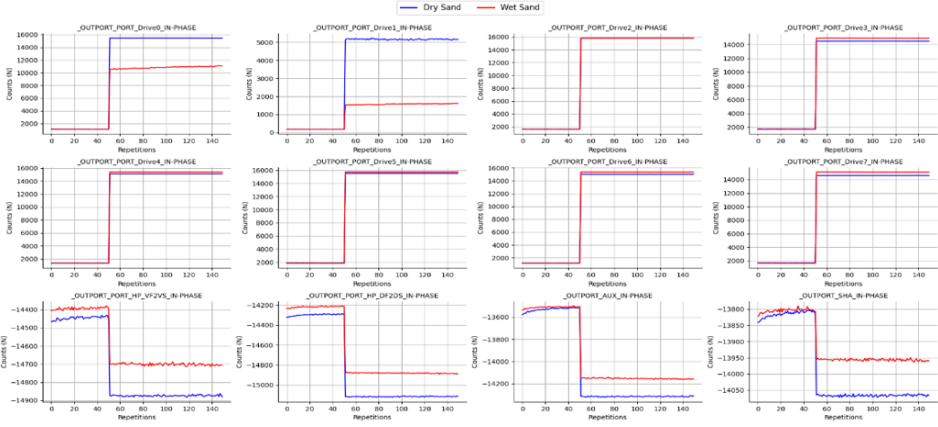


Fig. 21 Example of a measurement performed on a fine sand sample taken in Torvaianica. The blue line represents the dry sample, while the red line represents the wet sample.

As can be seen in Fig. 21, 12 sensors show a clear variation in the signal when the sand is wetted by water. The PORT\_Drive2, PORT\_Drive4 and PORT\_Drive5 sensors do not seem to register a significant variation in the signal when wet sand is inserted.

**B. MACHINE TRAINING**

Once the dataset was completed, we proceeded with the second phase of the work which consisted of analyzing the data using MLP and KNN machine learning algorithms.

The parameters used for MLP and KNN models have been collected in the following table Tab. 4.

Settings	Value
Anomaly threshold	600
Environmental Samples	51
Hidden Layer	64
Learning rate	0.001
Epoch	100
Filtered Window	5

Tab. 4 MLP and KNN models settings.

The MLP model performed in 7 classes (6 soils + darkness) had an average accuracy of 89.0 %, while the KNN model resulted in a global accuracy of 76.0 % and the results with the confusion matrices are summarized in Fig. 22 and Fig 23.

	BLACK-BOX	FINE-SAND	MEDIUM-SAND	COARSE-SAND	SILT	CLAY	LOAM
BLACK-BOX	100.0% ±0.0%	0.0%	0.0%	0.0%	0.0%	0.0%	0.0%
FINE-SAND	0.0%	84.3% ±31.4%	15.7%	0.0%	0.0%	0.0%	0.0%
MEDIUM-SAND	0.0%	11.9%	88.1% ±23.8%	0.0%	0.0%	0.0%	0.0%
COARSE-SAND	0.0%	1.1%	0.0%	98.9% ±2.2%	0.0%	0.0%	0.0%
SILT	0.0%	0.0%	0.0%	0.0%	54.3% ±14.2%	0.0%	35.7%
CLAY	0.0%	0.0%	0.0%	0.0%	0.0%	100.0% ±0.0%	0.0%
LOAM	0.0%	0.0%	0.0%	0.0%	11.4%	0.0%	88.6% ±22.7%

Fig. 22 MLP Model Confusion Matrix

	BLACK-BOX	FINE-SAND	MEDIUM-SAND	COARSE-SAND	SILT	CLAY	LOAM
BLACK-BOX	100.0% ±0.0%	0.0%	0.0%	0.0%	0.0%	0.0%	0.0%
FINE-SAND	0.0%	89.5% ±1.1%	0.5%	0.0%	0.0%	0.0%	0.0%
MEDIUM-SAND	0.0%	5.9%	77.3% ±36.7%	16.8%	0.0%	0.0%	0.0%
COARSE-SAND	0.0%	25.4%	50.8%	23.8% ±38.6%	0.0%	0.0%	0.0%
SILT	0.0%	0.0%	0.0%	0.0%	44.3% ±32.8%	0.0%	55.7%
CLAY	0.0%	0.0%	3.2%	0.0%	0.0%	96.8% ±0.6%	0.0%
LOAM	0.0%	0.0%	0.0%	0.0%	3.8%	0.0%	96.2% ±4.7%

Fig. 23 KNN Model Confusion Matrix

As can be observed on Fig. 22 and in Fig. 23, both models from a purely mathematical point of view seem to give good results in terms of accuracy of the single soil class analyzed.

## VII. DISCUSSION

The MLP and KNN models in Fig. 22 and in Fig. 23 yield very high accuracies, and test measurements performed with SLM-Studio confirmed the models' effectiveness. Indeed, by performing test measurements that replicate the same experimental conditions as the training measurements, the models recognize the soil class under consideration without confusion. The MLP and KNN models for a relatively low number of classes (6 classes + the background) gave practically similar results, in terms of soil class recognition, although probably by increasing the number of classes one will expect a greater discrepancy between the MLP and KNN model as shown in [66]. The model was tested on 2 test measures that replicated the same experimental conditions as the training phase.

1  
2  
3  
4  
5  
6  
7  
8  
9  
10  
11 Further tests on the model were performed by taking test measurements under experimental conditions slightly different  
12 from those used in training. For example, samples were analyzed containing water contents intermediate between the dry  
13 and wet conditions present in the model (for the wet condition, we used water-saturated soils). In this case, the model did  
14 not fully recognize the analyzed soil samples, except for soils with water contents practically close to saturation. This  
15 issue could be resolved in the future by enriching the dataset with measurements containing intermediate water contents,  
16 thus covering different concentrations ranging from anhydrous to fully saturated soil.

17 Finally, tests were performed on mixed samples, measuring different concentrations of sand, silt, and clay. The model  
18 being tested classified these soils, favoring larger grain sizes and sands. This implies that in the future, more quantitative  
19 investigation is needed to determine how these measurements can be improved by enriching the dataset.

## 18 VIII. CONCLUSIONS AND PERSPECTIVES

19 In this article, we collected information and data from literature with the aim of creating a dataset suitable for soil  
20 digitization. In addition to measurements describing the chemical and physical properties of soils, the paper aimed to add  
21 a dataset suitable for soil classification using a multispectral sensor, the SCP. This performs hyperspectral imaging  
22 measurements using 12 LEDs emitting in the spectral region ranging from VIS to NIR. From the dataset created for  
23 different soil classes, two machine learning models (MLP and KNN) were created, which yielded encouraging results in  
24 soil recognition using hyperspectral measurements as patterns. Considering what was discussed in the paper and  
25 considering the innovation we seek to convey through the development of a sensor for soil digitization, rather than  
26 discussing conclusions, we prefer to focus on perspectives.

26 The SCP multispectral sensor can be considered a low-cost solution that speeds up soil colorimetric analyses by  
27 facilitating, thanks to machine learning techniques, the classification of soil types based on grain size. Despite the  
28 instrumental limitations in recognizing soil with mixed grain size (sands with silts and clays), the sensor allows for faster  
29 analysis times because a simple measurement taken with SLM-Studio allows for the soil class to be determined, thus  
30 trying to eliminate the need for geological techniques such as sieving analysis and aerometric tests. In the future, this  
31 problem could be resolved by adding intermediate classes to the model with varying parameters as the grain sizes content.

31 This newly introduced tool can leverage multispectral imaging analysis to identify different soil types, reducing analysis  
32 times and simultaneously reducing data acquisition costs. The analyses carried out, although very promising and  
33 innovative, can still be considered preliminary and therefore open interesting perspectives. For example, in the future, it  
34 might be possible to apply SCP to the study of other soil mechanical properties, such as studying Atterberg limits at the  
35 colorimetric level. This would involve analyzing the interaction between fine-grained soil (silts and clays) and water and  
36 observing the four different physical states (solid, semi-solid, plastic, liquid) at the colorimetric level.

36 Another possible development of the SCP could be to connect the instrument to a portable device such as a smartphone  
37 on which SLM-Studio would be installed. This would make the instrument even easier to use in various work contexts,  
38 ranging from geology to precision agriculture.

38 Furthermore, we are considering adding a seismic sensor such as a Lennartz-3d-5s [67-68] to the SCP, which could be  
39 useful for characterizing the site effects of a given soil type and evaluating, for example, its resonance frequency the water  
40 content inside a terrain and carry out seismic micro-zonation analyses [69] by observing, for example, whether the same  
41 type of soil located in two different geological contexts can have a similar seismic response.

42 Even in this case, one could think of carrying out a measurement campaign covering different types of soil in Fig. 2 so as  
43 to have a seismic characterization of the different soils and then know the characteristics of the soil under examination by  
44 carrying out a seismic noise measurement lasting a few hours and, through machine learning [70], classify the soil and its  
45 physical characteristics.

## 45 ACKNOWLEDGMENT

46 I would like to thank Professors Fabio Cammarano and Francesco Basile of the Geophysics Laboratory of the Department  
47 of Geological Sciences at Roma Tre University for their assistance in sieving the soil samples. I also thank Professor  
48 Roberto Mazza of the Hydrogeology Laboratory and Professor Sveva Corrado of the Sedimentology Laboratory for their  
49 assistance in selecting the samples. I would like to thank Prof. Fabio Leccese of the Electrical and Electronic  
50 Measurements Laboratory for his technical support in the measurements performed with the SCP, and I would like to  
51 thank Sensichips s.r.l. for providing me with the instrumentation with which I carried out the work proposed in the paper.  
52 I also thank two students from the bachelor's degree program in Geological Sciences, Alessandro Lumaca, Gabriele  
53 Fontana, Michelangelo Greco and Sara Innocenti, for their assistance in obtaining a geological signature from the analysis  
54 of the soil samples collected and analyzed. I also thank the PhD student Giorgia Satta for having contributed in helping  
55  
56  
57  
58  
59  
60  
61  
62  
63  
64  
65

me with the soil sieving operations.

This work was co-funded by the European Union Horizon Europe program with the project URBAN M20 (GA 101180710).

#### REFERENCES

- [1] F. Fina, F. Leccese, "The LED's spectrophotometry in precision agriculture: A brief survey", *Acta IMEKO*, vol. 14 (2025) no. 1, pp. 1-15. DOI: [10.21014/actaimeko.v14i1.1970](https://doi.org/10.21014/actaimeko.v14i1.1970)
- [2] P. Musa, H. Sugeru, E. Prasetyo, "Wireless Sensor Networks for Precision Agriculture: A Review of NPK Sensor Implementations", *Sensors*, 2023, doi: <https://doi.org/10.3390/s24010051>
- [3] F. Leccese, "Remote-Control System of High Efficiency and Intelligent Street Lighting Using a ZigBee Network of Devices and Sensors," in *IEEE Transactions on Power Delivery*, vol. 28, no. 1, pp. 21-28, Jan. 2013, DOI: [10.1109/TPWRD.2012.2212215](https://doi.org/10.1109/TPWRD.2012.2212215).
- [4] F. Leccese, "A New Remote and Automated Control System for the Vineyard Hail Protection Based on ZigBee Sensors, Raspberry-Pi Electronic Card and WiMAX", *Journal of Agricultural Science and Technology*, 2023, B. 3. 853-864.
- [5] W. Bian, Y. Liu, Y. Wu, "A Bluetooth-Based Automated Agricultural Machinery Positioning System", *Electronics*, 13 (24), 4902, (2024), DOI: <https://doi.org/10.3390/electronics13244902>
- [6] J. Fournier-Sowinski, "Practical Handbook of Grain-Size Analysis Principles and methods", (2024), DOI: <https://doi.org/10.1016/j.biosystemseng.2010.03.013>.
- [7] G. López, "Grain Size Analysis", 2016 DOI: [https://doi.org/10.1007/978-1-4020-4409-0\\_18](https://doi.org/10.1007/978-1-4020-4409-0_18).
- [8] C. Di Stefano, V. Ferro, S. Mirabile, Comparison between grain-size analyses using laser diffraction and sedimentation methods, *Biosystems Engineering*, Vol. 106, Issue 2, 2010, Pag. 205-215, ISSN 1537-5110, DOI: <https://doi.org/10.1016/j.biosystemseng.2010.03.013>.
- [9] M. C. Magno, S. Barbizzi, P. De Zorzi, A. Pati, P. Leone, T. Guagnini, G. Pierfranceschi, "Proficiency Test on grain size measurements of marine sediments," *2023 IEEE International Workshop on Metrology for the Sea; Learning to Measure Sea Health Parameters (MetroSea)*, La Valletta, Malta, 2023, pp. 133-137, doi: <https://doi.org/10.1109/MetroSea58055.2023.10317114>
- [10] M. Celia Magno, F. Venti, G. Gaglianone, G. Pierfranceschi, E. Romano, Grain Size Analysis: A Comparison Between Laser Granulometer and Sedigraph, *MetroSea*, 2017.
- [11] [www.sensichips.com](http://www.sensichips.com) (Accessed in June 2025)
- [12] S. Hemedi, Geotechnical Engineering. *Advances in Soil Mechanics and Foundation Engineering*, (2020)
- [13] T. Lunne, P. Robertson, J. Powell, Cone Penetration Testing in Geotechnical Practice. *Soil Mechanics and Foundation Engineering*, 46, (1997) doi: 10.1007/s11204-010-9072-x.
- [14] C. Patel, S. Parmar, SPT, SCPT, and DCPT Correlation for SC, CL, and SM-SC Soils: A Case Study of Nadiad Soil, 2021, doi: 10.13140/RG.2.2.13923.07209.
- [15] E. Rolia, D. Sutjningsih, Dwita, Application of geoelectric method for groundwater exploration from surface (A literature study). *AIP Conference Proceedings*. 1977. 020018. Doi: 10.1063/1.5042874.
- [16] F. Cammarano, P. Mauriello, D. Patella, S. Piro, F. Rosso, L. Versino, Integration of high resolution geophysical methods. Detection of shallow depth bodies of archaeological interest, DOI: [10.4401/ag-4339](https://doi.org/10.4401/ag-4339)
- [17] L. Giorgi, G. Leucci, Passive and active electric methods: New frontiers of application, (2019), Doi:10.1016/B978-0-12-812429-1.00001-5
- [18] D. Corwin, J. Hendrickx, Electrical resistivity: Wenner array. *Methods of soil analysis part 4 physical methods*, 2002, 1282-1287.
- [19] A.B. Eluwole, M.O. Olorunfemi, L.S Adebisi, A Wenner array routine for optimum electrode spacing selection for resistivity measurements over thin subsurface media. *SN Appl. Sci.* 5, 112 (2023). Doi: <https://doi.org/10.1007/s42452-023-05332-9>
- [20] T. Rahmani, D. Sari, A. Akmam, H. Amir, A. Putra, Using the Schlumberger configuration resistivity geoelectric method to analyze the characteristics of slip surface at Solok. *Journal of Physics: Conference Series*, 2020, 1481. 012030. Doi: 10.1088/1742-6596/1481/1/012030.
- [21] K. Zajicová, T. Chuman, "Application of ground penetrating radar methods in soil studies: A review", *Geoderma*, Volume 343, 2019, Pages 116-129, ISSN 0016-7061, DOI: <https://doi.org/10.1016/j.geoderma.2019.02.024>.
- [22] D. Moret-Fernández, F. Lera, B. Latorre, J. Tormo, J. Revilla, "Testing of a commercial vector network analyzer as low-cost TDR device to measure soil moisture and electrical conductivity", *CATENA*, Volume 218, 2022, 106540, ISSN 0341-8162, DOI: <https://doi.org/10.1016/j.catena.2022.106540>.
- [23] K. Grote, S. Hubbard, Y. Rubin, "Field-scale estimation of volumetric water content using ground-penetrating radar

Field Code Changed

Field Code Changed

Field Code Changed

Field Code Changed

Field Code Changed

Field Code Changed

Field Code Changed

1  
2  
3  
4  
5  
6  
7  
8  
9  
10  
11  
12  
13  
14  
15  
16  
17  
18  
19  
20  
21  
22  
23  
24  
25  
26  
27  
28  
29  
30  
31  
32  
33  
34  
35  
36  
37  
38  
39  
40  
41  
42  
43  
44  
45  
46  
47  
48  
49  
50  
51  
52  
53  
54  
55  
56  
57  
58  
59  
60  
61  
62  
63  
64  
65

ground wave techniques: *Water Resources Research*”, Volume 39, (2023), DOI: <http://doi.org/10.1029/2003WR0245>

[24] E. Pettinelli, A. Di Matteo, S. E. Beaubien, E. Mattei, S. E. Lauro, A. Galli, G. Vannaroni, “A controlled experiment to investigate the correlation between early-time signal attributes of ground-coupled radar and soil dielectric properties”, *Journal of Applied Geophysics*, Volume 101, 2014, Pages 68-76, ISSN 0926-9851, DOI: <https://doi.org/10.1016/j.jappgeo.2013.11.012>.

[25] F. Adamo, F. Attivissimo, L. Fabbiano, N. Giaquinto, M. Spadavecchia, “Soil moisture assessment by means of compressional and shear wave velocities: Theoretical analysis and experimental setup, Measurement”, Volume 43, Issue 3, 2010, Pages 344-352, ISSN 0263-2241, DOI: <https://doi.org/10.1016/j.measurement.2009.11.007>.

[26] M. Pischiutta, F. Linsalata, A. Mercuri, F. Salvini, F. Fina, G. Cultrera, L. Minarelli, G. Di Giulio, “Rock-site amplification on topography at Introdacqua, Central Italy: a rock-fracturing effect?”, *Acta Geophys.* (2025), DOI: <https://doi.org/10.1007/s11600-024-01515-z>

[27] M. Pischiutta, A. Mercuri, F. Fina, F. Salvini, L. Minarelli, G. Cultrera, G. Di Giulio, “Passive seismic survey across the fault-zone of Introdacqua, central Italy: the subsurface geological structure role on the site amplification pattern”, EGU General Assembly 2024, Vienna, Austria, 14–19 Apr 2024, EGU24-18014, DOI: <https://doi.org/10.5194/egusphere-egu24-18014.2024>.

[28] H. Berger Roisenberg, F. Magrini, I. Molinari, L. Boschi, F. Cammarano, “Rayleigh wave attenuation and phase velocity maps of the greater Alpine region from ambient noise”, *Sci Rep* 14, 29164, (2024) , DOI: <https://doi.org/10.1038/s41598-024-80729-z>

[29] T. Dean, M. Grant, A beginner’s guide to seismic sensors. Preview, 2024, 38-44, doi: 10.1080/14432471.2024.2395647.

[30] M. Vassallo, G. Cultrera, G. Di Giulio, F. Cara, G. Milana, Peak frequency changes from HV spectral ratios in Central Italy: Effects of strong motions and seasonality over 12 years of observations. *Journal of Geophysical Research: Solid Earth*, 127, e2021JB023848, (2022), DOI: <https://doi.org/10.1029/2021JB023848>

[31] G. Cultrera, A. Mercuri, M. Vassallo, A. Bobbio, Antonella, G. Riccio, G. Di Giulio, (2025), TIME VARIATION OF H/V IN URBAN ENVIRONMENTS: THE SPQR EXPERIMENT IN ROME (ITALY).

[32] A. Almwaw, “Soil temperature Sensors in Agriculture and the role of Nanomaterials in Temperature Sensors Preparation”, (2018)

[33] Y. K. Kushwaha, R. K. Panigrahi, A. Pandey, “Performance analysis of capacitive soil moisture, temperature sensors and their applications at farmer’s field”, *Environ Monit Assess* 196 , 793 (2024). DOI: <https://doi.org/10.1007/s10661-024-12946-y>

[34] M. Nadporozhskaya, N. Kovsh, R. Paolesse, L. Lvova, “Recent Advances in Chemical Sensors for Soil Analysis: A Review”, *Chemosensors* 2022 , 10 , 35. DOI: <https://doi.org/10.3390/chemosensors10010035>

[35] U. B. Mahadevaswamy, N. Meghana, “Design and Development of Soil Moisture Sensor”, *International Journal of Innovative Technology and Exploring Engineering (IJITEE)* ISSN: 2278-3075 (Online), Volume-10 Issue-4, February 2021, DOI: <https://doi.org/10.35940/ijitee.D8438.021042>

[36] M. Mattia, G. Mondati, R. Mazza, C. Rosa, C. Di Salvo, P. Tuccimei, “Groundwater–River Water Interaction in an Urban Setting (Rome, Italy) Using a Multi-Method Approach (Hydrogeological and Radon Analyses)”, *Water* , 17 (10), 1555, (2025), DOI: <https://doi.org/10.3390/w17101555>

[37] P. Tuccimei, M. Soligo. “Correcting for Interference in Soil Radon Flux Measurements.” *Radiation Measurements* 43, no. 1 (2008): 102–5. DOI: <https://doi.org/10.1016/J.RADMEAS.2007.05.056>

[38] M. Vitelli, G. Cerro, L. Gerevini, G. Miele, A. Ria, M. Molinara, “SENSIPLUS-LM: A Low-Cost EIS-Enabled Microchip Enhanced with an Open-Source Tiny Machine Learning Toolchain”, *Computers*. 12. 23. DOI: <https://doi.org/10.3390/computers12020023>

[39] A. Ria, M. Cicalini, G. Manfredini, A. Catania, M. Piotto, P. Bruschi, “The SENSIPLUS: A Single-Chip Fully Programmable Sensor Interface”, In: Saponara, S., De Gloria, A. (eds) *Applications in Electronics Pervading Industry, Environment and Society* ApplePies 2021. Lecture Notes in Electrical Engineering, vol 866. Springer, (2022), DOI: [https://doi.org/10.1007/978-3-030-95498-7\\_36](https://doi.org/10.1007/978-3-030-95498-7_36)

[40] M. Leccisi, M. Greco, G. Schirripa Spagnolo, E. De Francesco, F. Leccese, "Low Cost Multispectral Sensor for Monitoring Vine Leaf Density," *2024 IEEE International Workshop on Metrology for Agriculture and Forestry (MetroAgriFor)* , Padua, Italy, 2024, pp. 86-91, DOI: <https://doi.org/10.1109/MetroAgriFor63043.2024.10948775> .

[41] M. Greco, E. Giovenale, F. Leccese, A. Doria, “A Discrimination of Healthy and Rotten Hazelnuts Using a THz Imaging Scanner”, 229-233, (2022), DOI: <https://doi.org/10.1109/MetroAgriFor55389.2022.9964672>.

[42] M. Greco, G. Schirripa Spagnolo, A. Lai, F. Bonfigli, E. Giovenale, F. Leccese, “Detection of Powdery Mildew Disease on Hazelnut Leaves by UV/VIS Fluorescence”, (2024), 92-96, DOI: <https://doi.org/10.1109/MetroAgriFor63043.2024.10948845>.

Field Code Changed

Field Code Changed

1  
2  
3  
4  
5  
6  
7  
8  
9  
10  
11  
12  
13  
14  
15  
16  
17  
18  
19  
20  
21  
22  
23  
24  
25  
26  
27  
28  
29  
30  
31  
32  
33  
34  
35  
36  
37  
38  
39  
40  
41  
42  
43  
44  
45  
46  
47  
48  
49  
50  
51  
52  
53  
54  
55  
56  
57  
58  
59  
60  
61  
62  
63  
64  
65

[43] C.A. Santos, M. Lopo, R. N. M. J. Páscoa, J. A. Lopes. "A Review on the Applications of Portable Near-Infrared Spectrometers in the Agro-Food Industry." *Applied Spectroscopy* 67, no. 11 (2013): 1215–33. DOI: <https://doi.org/10.1366/13-07228>.

[44] A. K. Mahlein, B. Arnal, G. Jayme, KS Chiang, E. M. Del Ponte, CH Bock, "From Detection to Protection: The Role of Optical Sensors, Robots, and Artificial Intelligence in Modern Plant Disease Management, Phytopathology", Vol 114, 1733-1741, 2024, DOI: <https://doi.org/10.1094/PHYTO-01-24-0009-PER>

[45] Y. Qm, W. Zhang, "Estimation of Leaf Water Content of Different Leaves from Different Species Using Hyperspectral Reflectance Data", *Annals of Agricultural Sciences*, Vol. 7, 1111-2022, (2024), DOI: <https://doi.org/10.26420/annagricropsci.2021.1111>.

[46] K. Zhang, W. Li, H. Li, Y. Luo, Z. Li, X. Wang, X. Chen, "A Leaf-Patchable Reflectance Meter for In Situ Continuous Monitoring of Chlorophyll Content", *Adv. Sci.* 2023, 10, 2305552. DOI: <https://doi.org/10.1002/advs.202305552>

[47] I. Kasajima, "Measuring plant colors", *Plant Biotechnology*, (2019), Vol 36, DOI: <https://doi.org/10.5511/plantbiotechnology.19.0322a>.

[48] N. Kirillova, T. Sileva, Colorimetric analysis of soils using digital cameras. *Moscow University Soil Science Bulletin*, Vol 72, 13-20, (2017) DOI: <https://doi.org/10.3103/S0147687417010045>

[49] F. Cammarano, M. Guerri, "Effects of Chemical Composition, Water and Temperature on Physical Properties of Continental Crust", *American Geophysical Union, Fall Meeting 2015*, abstract id. T11A-2863

[50] L. Scesi, M. Papini, P. Gattinoni, *Principi di Geologia Applicata*, ISBN: 978-88-08-18642-3

[51] K. Yin, A.L. Fauchille, E. Di Filippo, P. Kotronis, G. Sciarra, A Review of Sand–Clay Mixture and Soil–Structure Interface Direct Shear Test. *Geotechnics* 2021, 1, 260-306. <https://doi.org/10.3390/geotechnics1020014>

[52] V.A. Sakleshpur, M. Prezzi, R. Salgado, CPT-Based Design of Pile Foundations in Sand and Clay: Perspectives, 2023

[53] C. Lyu, Q. Sun, W. Zhang, Real - Time Geoelectric Monitoring of Seepage into Sand and Clay Layer. *Groundwater Monitoring & Remediation*, (2019), 39. Doi: 10.1111/gwmr.12352.

[54] E.V. Deshcherevskaya, O.V. Pavlenko, The Response of Sandy and Clayey Soils to Weak and Strong Seismic Motions. *Izv., Phys. Solid Earth* 59, 633–649 (2023). <https://doi.org/10.1134/S1069351323040043>

[55] J. Nam, S. Hong, Y. Lee, I. Kim, Correlation analysis between color and grain size of sand using a colorimeter, *Special Issue No. 114*, pp. 201–205. Coconut Creek (Florida), (2021), ISSN 0749-0208.

[56] C. Nolet, A. Poortinga, P. Roosjen, H. Bartholomeus, G. Ruessink, Measuring and Modeling the Effect of Surface Moisture on the Spectral Reflectance of Coastal Beach Sand. *PLoS one*. 9. e112151, (2014), doi: 10.1371/journal.pone.0112151.

[57] J. Torrent, V. Barrón, Laboratory measurement of soil color: Theory and practice. *SSSA Special Publication (Soil Science Society of America)*. 21-33, (1993)

[58] N.B. Prasad, *Groundwater Hydrology*, (2002)

[59] [Progetto CARG - Cartografia Geologica e Geotematica](https://progetto-carg.isprambiente.it/cartografiaCARG/index.php?source=cartageologica&regione=Lazio), site: <https://progetto-carg.isprambiente.it/cartografiaCARG/index.php?source=cartageologica&regione=Lazio>

[60] [374 ROMA.pdf](https://progetto-carg.isprambiente.it/cartografiaCARG/viewer.php?source=386_FIUMICINO_PREVIEW), doi: <https://doi.org/10.15161/oar.it/76970>

[61] [Progetto CARG - Cartografia Geologica e Geotematica](https://progetto-carg.isprambiente.it/cartografiaCARG/viewer.php?source=386_FIUMICINO_PREVIEW), 386 FIUMICINO\_PREVIEW, site: [https://progetto-carg.isprambiente.it/cartografiaCARG/viewer.php?source=386\\_FIUMICINO\\_PREVIEW](https://progetto-carg.isprambiente.it/cartografiaCARG/viewer.php?source=386_FIUMICINO_PREVIEW)

[62] [Progetto CARG - Cartografia Geologica e Geotematica](https://progetto-carg.isprambiente.it/cartografiaCARG/viewer.php?source=387_ALBANO_LAZIALE) 387\_ALBANO\_LAZIALE doi: <https://doi.org/10.15161/oar.it/73sy6-ztb78>

[63] A. Kayabasi, Ahmet, "MLP and KNN Algorithm Model Applications for Determining the Operating Frequency of A-Shaped Patch Antennas" *International Journal of Intelligent Systems and Applications in Engineering*. 3. 154-157., (2017), doi: <https://doi.org/10.18201/ijisae.2017531432>.

[64] J. Hosen, "Comparison of Regression, K-Nearest Neighbors (KNN) and Multi-Layer Perceptron (MLP) Models for the Prediction of Weight, Gender and Body Mass Index Status," *International journal of computer applications. Foundation of Computer Science*, (2023) doi: 10.5120/IJCA2023923040.

[65] G. Gandolfi, L. Paganelli, "Petrografia delle sabbie del litorale tirrenico fra i Monti dell'Uccellina e Monte di Procide, *Miner. Petrogr. Acta*, vol. 28, 1984, pp. 173-191

[66] H. Mustafa, M. Vitelli, F. Milano, M. Molinara, L. Ferrigno, A. Ria, F. Fina, F. Leccese, "Evaluation of Deep Learning Models for State of Charge Estimation for Lithium Batteries Using Image-Encoded Electrochemical Impedance Spectroscopy Data," *2025 IEEE International Workshop on Metrology for Automotive (MetroAutomotive)*, Parma, Italy, 2025, pp. 62-67, doi: 10.1109/MetroAutomotive64646.2025.11119254.

[67] F. Dammeyer, J. Moore, F. Haslinger, S. Loew, "Characterization of alpine rockslides using statistical analysis of seismic signals", *Journal of Geophysical Research (Earth Surface)*, 2011, doi: 10.1029/2011JF002037.

[68] C. Acerra, G. Alguacil, K. Atakan, R. Azzara, P.Y. Bard, F. Blarel, F. Cara, P. Teves-Costa, A.M. Duval, B. Guillier,

Field Code Changed

Field Code Changed

Field Code Changed

1  
2  
3  
4  
5  
6  
7  
8  
9  
10  
11  
12  
13  
14  
15  
16  
17  
18  
19  
20  
21  
22  
23  
24  
25  
26  
27  
28  
29  
30  
31  
32  
33  
34  
35  
36  
37  
38  
39  
40  
41  
42  
43  
44  
45  
46  
47  
48  
49  
50  
51  
52  
53  
54  
55  
56  
57  
58  
59  
60  
61  
62  
63  
64  
65

M. Grandison, J. Havskov, M. Ohrnberger, S. Rao, N. Theodoulidis, E. Tvedt, T. Utheim, S. Vidal, S. Zacharopoulos, (2002). Site Effects Assessment Using Ambient Excitations. Doi: 10.13140/2.1.4909.9204.

[69] F. Cara, G. Cultrera, G. Riccio, *et al.* Temporary dense seismic network during the 2016 Central Italy seismic emergency for microzonation studies. *Sci Data* **6**, 182 (2019). DOI: <https://doi.org/10.1038/s41597-019-0188-1>

[70] S.M. Mousavi, G. C. Beroza, "Machine Learning in Earthquake Seismology", "Annual Review of Earth and Planetary Sciences", (2023), Vol. 51, pp 105-129, DOI: <https://doi.org/10.1146/annurev-earth-071822-100323>

